Predicting Variation in Thermal Infrared Intrusion Detection

Security Technology 049, Session V, Group I

Lindamae Peck* and James Lacombe

US Army Engineer Research and Development Center
Cold Regions Research and Engineering Laboratory
72 Lyme Road
Hanover, NH 03755

Telephone: (603) 646 4261

FAX: (603) 646 4397

E-mail: lpeck@crrel.usace.army.mil

Predicting Variation in Thermal Infrared Intrusion Detection

Lindamae Peck and James Lacombe

US Army Engineer Research and Development Center
Cold Regions Research and Engineering Laboratory (CRREL)
72 Lyme Road, Hanover, NH 03755

ABSTRACT

The detection capability of passive infrared (PIR) intrusion detection systems under a broad range of site conditions is estimated from predictions of the intruder's thermal contrast. The Intruder Thermal Model (ITM), developed at CRREL, predicts the surface temperature of a person through an energy balance approach that accounts for metabolic rate and sensible and latent heat transfer due to respiration, evaporation, convection, and radiation. A second model, developed under the Smart Weapons Operability Enhancement JT&E, predicts the thermal background as a function of ground cover, weather, and terrain. Together, ITM output and background temperatures (modeled or measured) provide the information necessary to predict an intruder's thermal contrast, from which the effectiveness of PIR sensor systems under the specified sensor site conditions can be assessed.

INTRODUCTION

Thermal contrast is fundamental to the effectiveness of passive infrared (PIR) sensor systems for intrusion detection. Unless the intruder thermally 'stands out' from his background, he will pass undetected. The minimum thermal contrast required for reliable detection depends on a PIR's alarm criteria, which in turn typically depend on an operator-selectable sensitivity.

Standard procedure is to determine the appropriate sensitivity setting from a combination of trial intrusions and extended monitoring. The results of trial intrusions determine the PIR's probability of detection (P_d) for the system sensitivity, intruder characteristics, and site conditions in effect during the trials. Extended monitoring documents the likelihood of non-intruder alarms under the same conditions. A limitation of this approach to maintaining awareness of current PIR detection capability is that intrusion trials must be repeated for each significant change in site conditions in order to verify that the PIR's P_d continues to meet security requirements.

Alternatively, PIR detection capability under a broad range of site conditions and intruder activity could be estimated from predictions of the intruder's thermal contrast. This paper presents predictions of thermal contrast obtained from modeling both the intruder's surface temperature and the thermal background, and proposes guidance on avoiding invalid reliance on PIR systems under site conditions when the probability of detecting an intruder is low.

MODELS

Intruder Thermal Model (ITM). The ITM, developed at CRREL, provides steady-state predictions of the average surface temperature of an intruder in terms of his height, weight, and activity, and the thermal properties of his clothing. ITM accounts for metabolically generated heat and heat exchange with the environment via conduction, convection, perspiration, and respiration. It also accounts for long- and short-wave radiation exchanges with the environment. The intruder's assumed metabolic rate is based on the speed at which he is walking or running, which is specified by the user. ITM determines sensible and latent heat transfer through the intruder's clothing by having the user select one of three seasonally appropriate clothing ensembles (summer, spring/fall, or winter garments). A full description of ITM and its validation is given in Lacombe and Peck (2000).

Table 1. ITM site-specific inputs.

Latitude, longitude, time zone	Relative humidity (%)
Julian date, 24-hour time	Incoming longwave radiance (W/m^2)
Air temperature (°C)	Incoming solar radiance (W/m^2)
Ground surface temperature (°C)	Wind speed (m/s)
Barometric pressure (mbar)	

The complete set of ITM inputs is listed in Table 1; the intruder is assumed to be a perfect infrared emitter (emissivity = 1). Barometric pressure and ground surface temperature are relatively minor factors for which reasonable estimates are adequate; ground surface (background) temperature, however, is fundamental in predicting the intruder's thermal contrast. The same ground surface temperature should be used in both ITM calculations and thermal contrast calculations, i.e., intruder temperature minus background temperature. The inclusion of the short-wave solar contribution to the overall heat balance is notable; usually, only long-wave radiation exchange is considered, which greatly limits the applicability of such an approach to outdoor situations, particularly when sunny daytime conditions are being modeled. ITM models solar heating by representing the intruder as a cylinder, with the top surface of the cylinder being the upper horizontal surfaces of the intruder (his head and shoulders) and its vertical cross-sectional area being his profile.

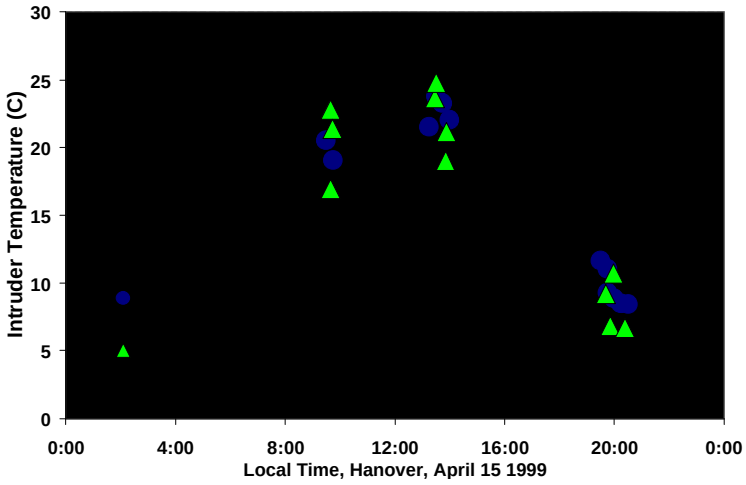

Figure 1. ITM predictions of body-averaged surface temperature vs. infrared measurements.

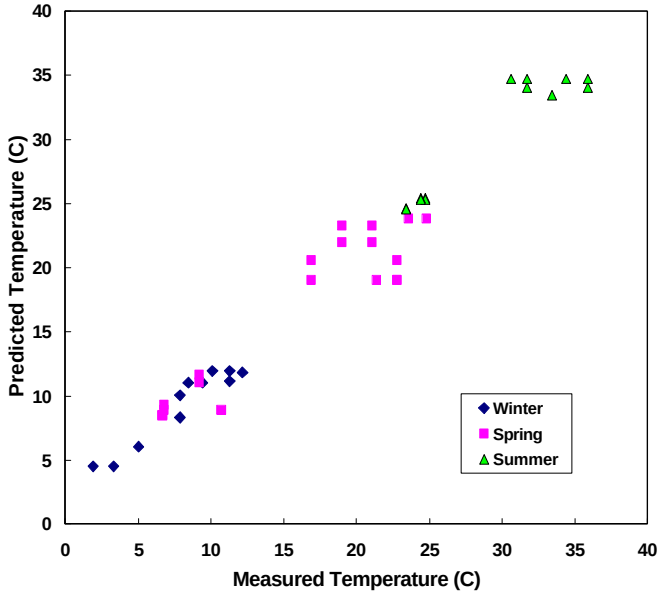

Figure 2. Summary plot showing measured vs. predicted intruder surface temperatures for different seasons.

ITM predictions have been compared with calibrated thermal imagery of an intruder to establish how well the model performs. The thermal imagery was recorded at the CRREL intrusion detection system field site in Hanover, New Hampshire, in spring, summer, and winter 1999 - 2000. Concurrent weather data were obtained from a nearby meteorological station. Intruder body-averaged surface temperatures were extracted from the thermal imagery using image analysis software. Samples of measured and calculated results are presented in Figure 1; they correspond to three thermal imaging sessions (morning, early afternoon, evening) conducted on 15 April 1999. On this day the skies were mostly clear, winds were light, and air temperatures ranged between -1 and +14°C. Agreement between ITM predictions and measured surface temperatures is reasonably good. All intruder surface temperatures from thermal imagery (15 April 1999, 27 July 1999, 15 March 2000) are plotted in Figure 2 against corresponding ITM predictions for the same time periods. These results indicate that ITM

provides realistic representations of both daily and seasonal fluctuations in average intruder surface temperature.

Background temperature. Simulations of the physical temperatures of a variety of groundcovers as a function of weather conditions were generated using the Smart Weapons Operability Enhancement (SWOE) computer codes (e.g., Welsh and Palmer, 1991). The SWOE inputs include those required by ITM (Table 1), plus wind direction, visibility, aerosol type (if present), precipitation amount and type, cloud data (fractional cloud cover and cloud type at low, middle, and high bands), direct and diffuse components of incident solar radiation, solar zenith and azimuth, and soil temperature profile.

For the SWOE simulations, the surface material was silt (bare ground), snow, or grass. The standard snow depth for SWOE calculations, 5 cm, was retained for this project. The grasscover was represented as a uniform distribution of 7.5-cm-tall grass blades. The grass's solar radiation absorption was specified to vary with the season to represent more absorption by green growing grass (0.8 spring, 0.85 summer, 0.75 autumn) and less absorption by brown, dormant grass (0.7 winter). Simulations were done with three vegetation densities, 20, 50 and 90%; the denser the vegetation cover, the less exposed to solar radiation the underlying soil is. Each vegetation simulation predicted the temperature of the grass blades and also the surface temperature of the exposed soil (the 80, 50 or 10%, respectively, of the surface that is not covered by grass blades). All the grass blades are predicted to be the same temperature; that temperature does not depend on how densely the grass blades cover the soil. The effective temperature of grasscovered ground is calculated from the predicted soil and grass blade temperatures in proportion to the density of the vegetation cover. All the surfaces were designated as level (no variation in elevation), with uniform exposure to solar radiation. The results were five sets of predicted surface temperatures for each weather scenario, i.e., bare ground, snowcover, 20% vegetation cover, 50% vegetation cover, and 90% vegetation cover.

Table 2. Weather scenarios for ITM and SWOE simulations.

Vermont			Yuma		
Day	Julian date	Air temperature: max, min (°C)	Day	Julian date	Air temperature: max, min (°C)
15 Jan 92	15	-7.4; -14.5	19 Mar 93	78	28.9; 12.4
16 Jan 92	16	-13.9; -19.0	22 Mar 93	81	30.3; 13.9
17 Jan 92	17	-9.4; -20.4	27 Mar 93	86	18.4; 8.4
04 Feb 92	35	-3.2; -12.3	05 Apr 93	95	23.7; 14.5
05 Feb 92	36	-4.6; -8.9	29 Apr 93	119	35.4; 18.7
18 Feb 92	49	6.8; -3.9			
19 Feb 92	50	5.7; 1.4	22 Jul 92	203	28; 39
29 Apr 92	119	18.5; -1.3	22 Jul 93	203	24; 39
30 Apr 92	120	17.9; 0.4			
01 Jul 92	182	24.3; 10.6			
02 Jul 92	183	22.1; 5.9			
03 Jul 92	184	17.8; 6.7			

WEATHER SCENARIOS

Data from SOROIDS, CRREL's former physical security field site in South Royalton, Vermont, were used in both ITM and SWOE simulations (Table 2). Measured incident solar radiation on these days is shown in Figure 3. The winter periods represent various combinations of sunny and overcast mid- to late-winter days. The two April days represent transitional (end-of-winter) conditions in northern New England, when the range in air temperature over 24 hours is large; they also represent mid-winter conditions at locations that experience only mild winters. April 30 is particularly interesting because of the abrupt changes in sky condition from clear to overcast in early afternoon, and the impact of this on solar heating of the ground

cover and the intruder. The July period represents temperate mid-summer conditions on sunny and overcast days.

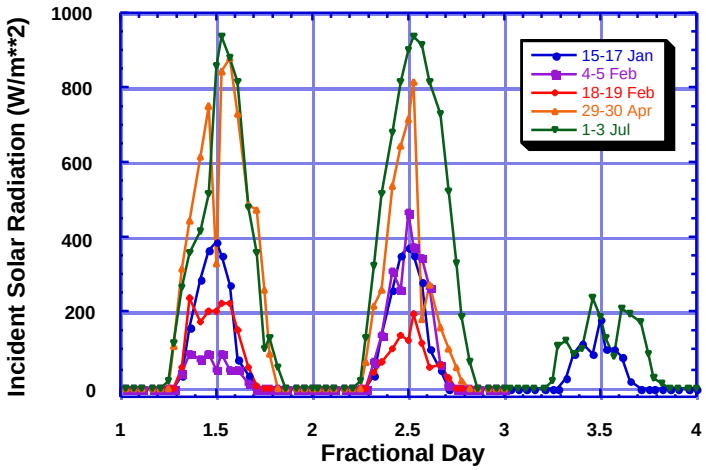

Figure 3. Measured incident solar radiation at the Vermont site. Day 1 is 15 Jan, 4 Feb, 18 Feb, 29 Apr or 1 Jul.

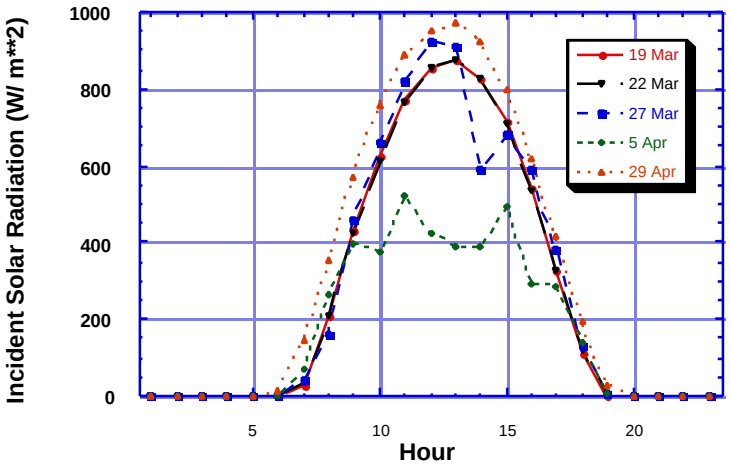

Figure 4. Measured incident solar radiation at the SWOE site in Yuma.

ITM simulations were also done based on desert conditions at Yuma, Arizona. Only intruder surface temperatures were predicted for this set of scenarios; the temperature of the background groundcover was measured radiometrically. The March and April 1993 data (meteorological and groundcover temperature) were acquired as part of the SWOE field experiment; incident solar radiation is plotted in Figure 4. The July 1992 and July 1993 data were provided by the US Army Engineer Research and Development Center, Topographic

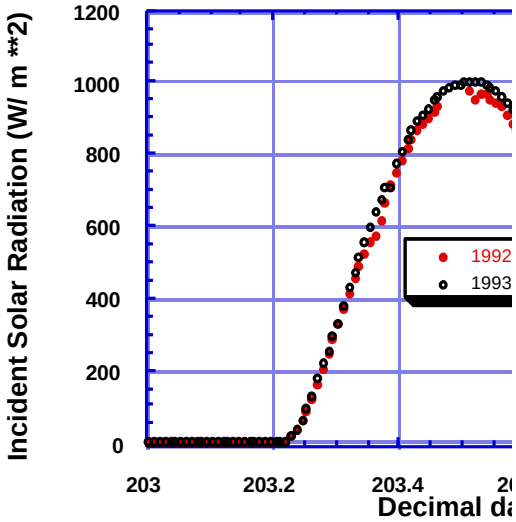

Figure 5. Measured incident solar rad

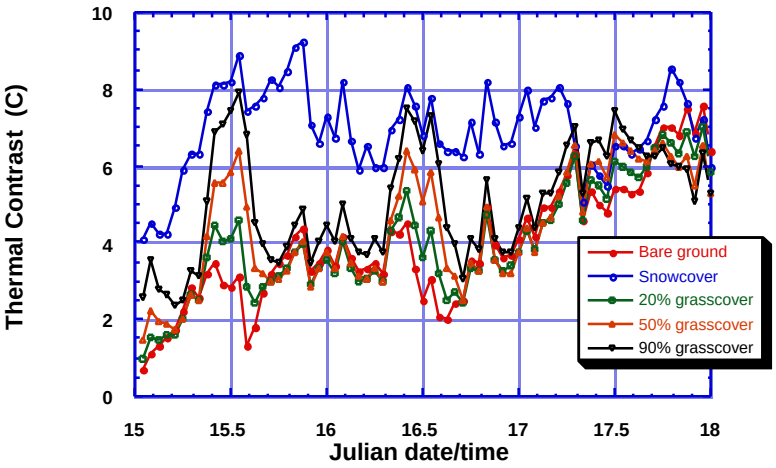

Figure 6. Intruder's thermal contrast with bare ground, snow or grasscover under the Vermont site conditions. a: 15 - 17 January.

Engineering Center (TEC); incident solar radiation is plotted in Figure 5. The SWOE ground surface temperatures correspond to a gravelly sand with no grass; the TEC ground surface temperatures correspond to either interdune grass or bare soil.

PREDICTED INTRUDER THERMAL CONTRAST

The intruder's thermal contrast is calculated by subtracting the temperature of the groundcover (measured or SWOE-predicted) from the ITM-predicted average body temperature. ITM accounts for both clothing-covered areas of the body and exposed skin, the temperature of the skin often being much greater than that of the clothing. The amount of exposed skin generally will be a small percentage of the intruder's total surface area, however, and so PIR detection will depend primarily on the average thermal contrast. In all the ITM simulations, the intruder is assumed to be walking at a speed of 1 m/s.

Winter (January, February). Thermal contrast under winter conditions (Figures 6 a, b, c) shows great variability from hour to hour, depending on the weather and on the type of groundcover (bare ground, snow, or grasscover of 20, 50 or 90% vegetation density). The largest thermal contrast is almost always associated with the snowcover, whereas the least thermal contrast during daylight hours is associated with the bare ground, which solar heats and radiationally cools more readily than do the grasscovers. Note that it is incorrect to assume that a snowcover will always be favorable for thermal infrared intrusion detection; Peck and Lacombe (1999) present effective countermeasures to passive infrared detection against a snowcover.

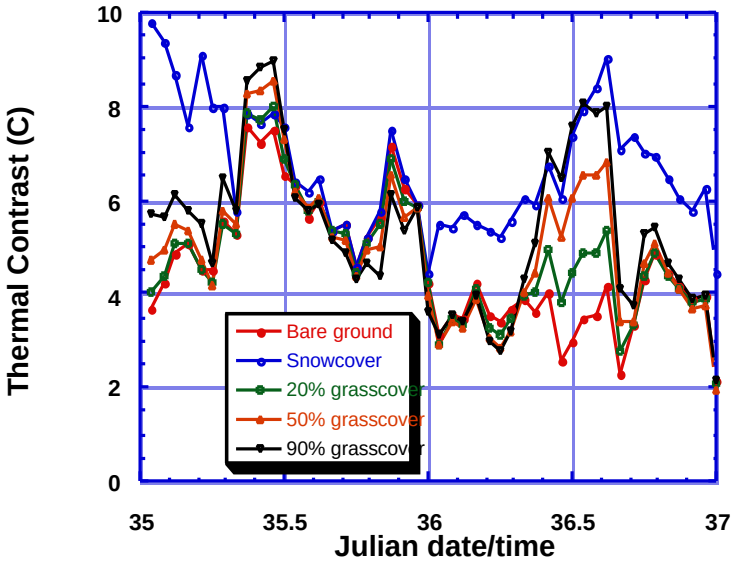

Figure 6b. 4 - 5 February.

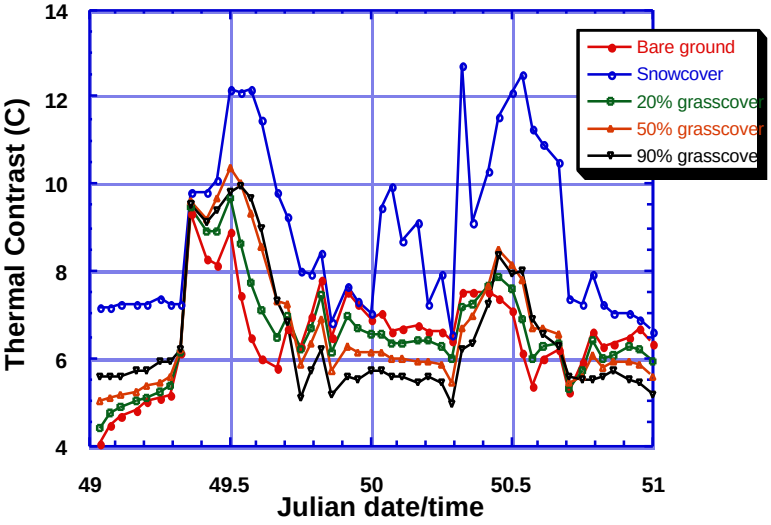

Figure 6c. 18 - 19 February.

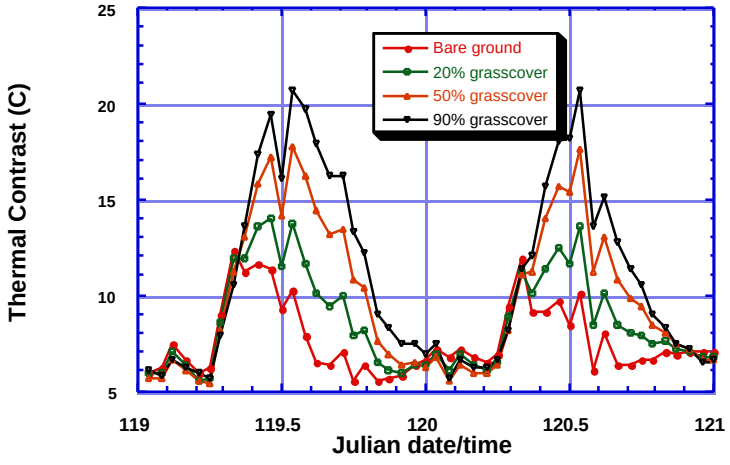

Figure 6d. 29 - 30 April.

On 17 January the sky is overcast following two sunny days. The surface temperatures of all the groundcovers are predicted to be within 2°C of each other during the daytime, so the range in thermal contrast at a given time is quite small compared to the earlier days. The thermal contrast is largely independent of groundcover.

On 4 - 5 February the situation is reversed, with the first day being overcast and the second day being sunny. During daytime on 5 February, the bare ground is the warmest, but the snowcover is not consistently the coldest groundcover. The 90% grasscover is predicted to be as cold as the snowcover for a few hours near mid-day; consequently, the intruder's thermal contrast will be similar with both that grasscover and the snowcover. The ordering of thermal contrasts during the day on 5 February is consistent with the relative solar heating of the groundcovers: thermal contrast is least with bare ground, because the soil responds most readily to solar heating and so is closest to the temperature of the intruder's clothing; next highest thermal contrast is with the 20% grasscover, which of all the grasscovers has an effective temperature closest to that of bare ground because of its greater amount of exposed soil; next highest thermal contrast is with the 50% grasscover, which, having denser vegetation, remains cooler than the 20% grasscover; and finally the highest thermal contrast is associated with the coolest groundcovers (90% grasscover, snowcover).

On the evening of 18 - 19 February, the thermal contrast is notable for its dependence on density of the grasscover. The bare ground, which had been the hottest groundcover during daylight hours on 18 February, at night cools to a lower temperature than any of the grasscovers. This leads to a reversal in the relative magnitudes of thermal contrasts among the non-snow groundcovers: thermal contrast in daytime is lowest with the hot soil , but

thermal contrast at night is highest with the cool soil. At night the densest vegetation results in the least thermal contrast because it cools the least of the three grasscovers.

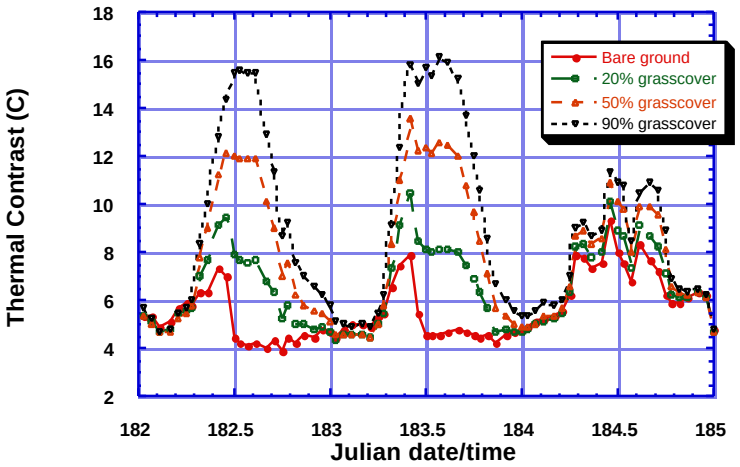

Figure 6e. 1 - 3 July.

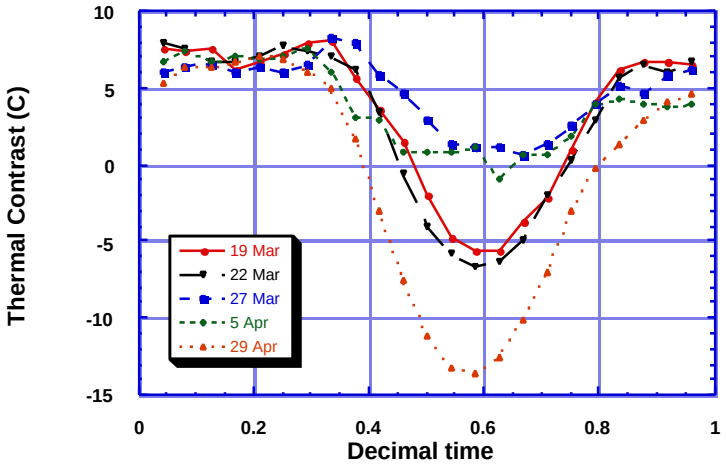

Figure 7a. Intruder's thermal contrast with gravelly sand (no grass) at SWOE site in Yuma.

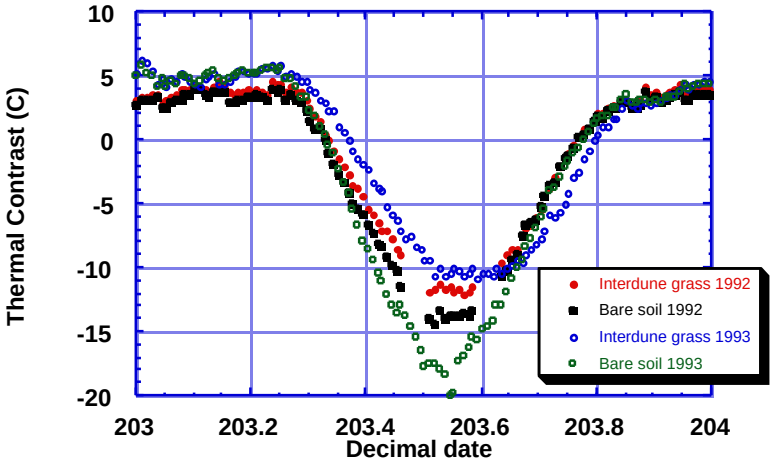

Figure 7b. Intruder's thermal contrast with interdune grass and with bare soil at the TEC site in Yuma.

In general, the bare ground is most likely to track the temperature swings of the intruder's surface caused by fluctuations in solar heating. This results in persistently low thermal contrast when the intruder is viewed against bare ground. Whether the surface temperature of a grasscover tracks the intruder's temperature swings depends on the density of its grass blades; the lower the density of grass blades, the less the difference is in temperature between the grasscover and either the bare ground or the intruder, and the smaller is his thermal contrast. Overall, the range in thermal contrast at a given hour is 0 to 6°C under winter conditions for backgrounds of bare ground, snowcover, or grasscover (20, 50 or 90% vegetation density).

Transitional period (March, April). In the Yuma desert on days with strong solar radiation (19 March, 22 March, 29 April), peak ground temperatures (measured) are 40 to 50°C, while peak intruder temperatures (predicted) are between 35 and 40°C. This results in negative daytime thermal contrasts of up to 15°C (Figure 7a). At night the ground cools more than does the intruder, resulting in strong positive thermal contrasts. Overall, the thermal contrast is at least 5°C (positive or negative) for most of a 24-hour period. On days marked by either low solar radiation (5 April) or persistent wind (27 March), both ground and intruder are much cooler during the daytime, approximately 25 to 30°C. The result is a protracted period when the calculated daytime thermal contrast is less than ±2°C.

Under northern New England conditions (29, 30 April), maximum solar radiation on sunny days is comparable to that at Yuma, but the corresponding ground surface temperature is much less, ranging from 23°C for bare soil to 10°C

for dense grasscover (90% vegetation cover). Thermal contrast (Figure 6d) shows pronounced diurnal cycles. At night there is little difference in thermal contrast with bare ground or grass-covers (conditions do not support a

snowcover) because all the groundcovers cool to approximately the same surface temperature; during daytime, the denser the vegetation, the greater is the thermal contrast, as the result of the vegetation inhibiting the heating of the grasscover. Daytime thermal contrasts range from ~5 to 21°C, depending on groundcover; nighttime thermal contrasts are on the order of 5 to 8°C.

The change in surface temperature in response to the abrupt drop in incident solar radiation in the afternoon of 30 April depends on the groundcover. The initial decrease in groundcover surface temperature ranges from ~5°C for the bare ground to ~1.5°C for the densest grasscover; the intruder's clothing initially cools by ~8°C. Because the 90% grasscover cools the least at the onset of overcast conditions, the decrease in thermal contrast is greatest for that groundcover.

Summer (July). Under northern New England summer conditions, thermal contrast (Figure 6e) on sunny days (1 - 2 July) depends strongly on the amount of vegetation cover, i.e., the more exposed soil per unit area of grasscover, the higher the grasscover's effective surface temperature and the lower its thermal contrast with clothing that is heated both by conduction from the intruder's body and absorption of solar energy. On overcast days (3 July), there is less range in thermal contrast because the surface temperatures of all the groundcovers cluster more closely during the daytime. The maximum temperatures of the densest grasscover on the three days differ by less than 2°C; the significant difference in thermal contrast on the third day arises from the intruder being cooler (maximum temperature ~6°C lower) because of weaker solar heating on an overcast day. Maximum daytime thermal contrasts range from 4 to 16°C; nighttime thermal contrasts are on the order of 5°C.

In the Yuma desert in July, peak surface temperatures (measured) range from 50 to 52°C for interdune grass to 54 to 62°C for the bare soil, much greater than the 29°C maximum predicted temperature for bare soil in northern New England. Desert groundcover temperatures fall to 24 to 28°C at night, versus a predicted minimum of 6°C under cooler northern New England weather conditions. The intruder's thermal contrast (Figure 7b) with the desert soil is twice that (in magnitude) of the New England soil, but opposite in sign. The desert daytime advantage is absent at night, when both the desert and the non-desert weather conditions result in predicted thermal contrasts on the order of 5°C for all the groundcovers.

SUMMARY

Predicted thermal contrasts obtained from simulated intruder temperatures and predicted or measured groundcover surface temperatures support the following observations and recommendations.

1) An intruder's thermal contrast with a snowcover is not necessarily consistently greater than that with a grasscover or bare soil; however, it is recommended that a PIR device be sited to view snow-covered ground whenever feasible in order to take advantage of those weather-dependent instances when the intruder's thermal contrast with the snowcover is higher (by up to 5°C in the scenarios studied). A snowcover is also favorable for passive infrared intrusion detection because PIRs viewing a snowcover typically can be operated at high sensitivity without incurring the penalty of numerous nuisance alarms.

2) Under temperate conditions, the intruder's thermal contrast is positive for a variety of groundcovers (bare ground, snow, grasscover) and seasonally different weather conditions (winter, transitional, summer). His daytime thermal contrast typically is least with bare soil, which more closely tracks the environmentally induced changes in the temperature of the intruder's clothing. To maximize an intruder's thermal contrast, a PIR should be sited to view a grasscover rather than bare soil, with dense grasscover being more favorable than a sparse grasscover. If the grasscover is long enough to blow in the wind, however, then during the daytime the PIR may need to be operated at relatively low sensitivity to avoid nuisance alarms. Probability of detection may remain high during daytime despite a low sensitivity setting because of the intruder's (predicted) large thermal contrast. Optimum system performance, however, can be expected if the PIR's detection zone has a well-maintained (i.e., frequently mowed) grasscover.

3) Under desert conditions, the intruder's thermal contrast is typically strongly negative during the day and relatively weakly positive at night. The exception is when solar heating of the groundcover and intruder's clothing is inhibited by either overcast sky condition or steady wind; under such conditions, the intruder's daytime thermal contrast can be close to 0°C. Bare soil is favorable over vegetated ground in terms of higher thermal contrast and probably lower incidence of nuisance alarms.

The above recommendations for siting a PIR to optimize intrusion detection do not take into account the spatial variability of thermal radiance from the various groundcovers. Depending on weather conditions and the types of groundcover within a PIR's field of view, nuisance alarms may be so numerous as to force a compromise between high thermal contrast and low nuisance alarm rate when siting a PIR.

ACKNOWLEDGMENTS

Support for this study was from the DTRA-funded Weather Vulnerability Assessment Tool project and CRREL's Winter Terrain Effects on Army Simulations program. The authors thank Dr. G. Koenig and Gary Koh for thoughtful technical reviews.

REFERENCES CITED

Lacombe, J. and L. Peck (2000). Modeling Surface Temperatures of Human Targets for Unattended Infrared Intrusion Detection. In: Proceedings, Unattended Ground Sensor Technologies and Applications, AeroSense 2000: 14th Annual International Symposium on Aerospace/Defense Sensing, Simulation and Controls, 24-28 April 2000, Orlando, FL.

Peck, L. and J. Lacombe (1999). Environmentally Dependent Countermeasures to Passive Infrared Detection. In: Proceedings of the 1998 Meeting of the IRIS Specialty Group on Camouflage, Concealment and Deception, 1-3 December 1998, Charleston, SC, p. 75 – 87.

Welsh, J. P. and R. A. Palmer (1991). Smart Weapons Operability Enhancement (SWOE) Program Joint Test and Evaluation Feasibility Study. SWOE Report 91-16.